Ege Coğrafya Dergisi 26 (2), 2017, 151-161, İzmir-Türkiye
Aegean Geographical Journal, 26 (2), 2017, 151-161, İzmir-TURKEY

ARAŞTIRMA MAKALESİ / RESEARCH ARTICLE

MODELING ABOVE GROUND BIOMASS IN CALABRIAN PINE FORESTS OF DÜZLERÇAMI (ANTALYA)

Düzlerçamı Kızılçam Ormanında (Antalya) Toprak Üstü Orman Biyokütlesinin Modellenmesi

Doğukan Doğu YAVAŞLI[1]

Ahi Evran Üniversitesi Fen – Edebiyat Fakültesi
Coğrafya Bölümü Kırşehir
dogukan.yavasli@ahievran.edu.tr

M. Kirami ÖLGEN

Ege Üniversitesi Edebiyat Fakültesi
Coğrafya Bölümü İzmir
kirami.olgen@ege.edu.tr

(Teslim: 1 Kasım 2017; Düzeltme: 11 Aralık 2017; Kabul: 20 Aralık 2017)

(Received: November 1, 2017; Revised: December 11, 2017; Accepted: December 20, 2017)

Abstract

Estimation of forest biomass is needed for monitoring the changes in carbon stocks as well as other purposes. This study reports on a test of the ability to estimate above ground biomass of Calabrian pine forests of Düzlerçamı, Antalya, Turkey using Landsat and ICESat/GLAS data. The field data has been collected in 2017 and plot-level estimates were calculated using the allometric equations. GLAS parameters and various Landsat vegetation indices were modeled using multiple regression analysis to estimate above ground biomass. In the first model ($Model_A$) height of median energy (HOME) and the ratio of HOME to maximum vegetation height (%HOME) parameter of GLAS showed relation with field based estimates of above ground biomass with a coefficient of determination (R^2) of 0.87. Above ground biomass derived from $Model_A$ and the variables obtained from Landsat indices has been used at the second model ($Model_B$) had a R^2 of 0.52 meaning the GLAS data is poorly correlated with Landsat at the study area. A better statistical relationship has been found with Landsat data and AGB with a R^2 of 0.91 in $Model_C$ that uses Landsat pixel values of each bands and pixel values of the indices are used as independent variable to explain above ground biomass. The results demonstrate a current potential for above ground biomass estimation of forests using optical sensor data and satellite lidar where airborne lidar data is not widely available.

Keywords: Above ground biomass, forest, ICESat/GLAS, Landsat

[1] Sorumlu Yazar/ Corresponding author: Doğukan Doğu YAVAŞLI / dogukan.yavasli@ahievran.edu.tr

Öz

Karbon stoklarındaki değişimlerin izlenmesi ile birlikte çeşitli diğer amaçlar için orman biyokütlesinin belirlenmesine ihtiyaç duyulmaktadır. Bu çalışma Düzlerçamı kızılçam ormanında (Antalya) toprak üstü orman biyokütlesinin Landsat ve ICESat/GLAS verileri kullanarak belirlenebilmesini test etmektedir. 2017 yılında arazi çalışmaları ile örneklem alanlarından toplanan veriler ile allometrik eşitlikler kullanılarak gerçek biyokütle verileri hesaplanmıştır. Toprak üstü orman biyokütlesinin modellenmesinde çok değişkenli regresyon analizi ile GLAS parametreleri ve çeşitli Landsat vejetasyon indekslerinden yararlanılmıştır. Birinci modelde ($Model_A$) GLAS verisinden medyan enerjinin yüksekliği (HOME) ve HOME'un maksimum yüksekliğe oranı parametrelerinin araziden toplanan biyokütle verileri ile olan ilişkisinde determinasyon katsayısı (R^2) 0.87 olarak tespit edilmiştir. $Model_A$'dan elde edilen toprak üstü orman biyokütlesi ile çeşitli Landsat indekslerinin kullanıldığı ikinci modelde ($Model_B$) 0.52 bulunan R^2 değeri GLAS verisinin çalışma alanında Landsat veriler ile zayıf bir korelasyonu bulunduğunu göstermiştir. Toprak üstü orman biyokütlesini açıklamak için Landsat indeks değerlerinin bağımsız değişken olarak kullanıldığı $Model_C$'de ise 0.91 R^2 ile istatistiksel olarak daha anlamlı bir istatistiksel ilişki belirlenmiştir. Sonuçlar toprak üstü orman biyokütlesinin belirlenmesinde hava lidar verilerinin bulunmadığı durumlarda optik sensörlerin ve uydu tabanlı lidar verilerin güncel potansiyelini göstermektedir.

Anahtar Kelimeler: Toprak üstü biyokütle, orman, ICESat/GLAS, Landsat

1. Introduction

Above ground biomass (AGB) that refers to all living biomass which is located above the ground is an essential ecological variable since forests remove carbon dioxide from the atmosphere. On the other hand, the carbon that constitutes approximately half of its biomass can easily transferred to atmosphere by fires, logging, climatic effects and the changes in land use activities. The increasing interest of AGB studies arise from its significance for atmospheric CO2 concentration and climate change in relation to that.

Estimation of AGB is traditionally practiced by harvesting all plant material within a plot, drying and weighing (Brown, 1997). The high cost, and destructive sampling have lead researchers to benefit from empirical allometric models that uses biometric measurements for calculation of biomass values (Chave et al., 2014). The integration of remote sensing with field assessments of AGB overcome the limited geographic coverage of these measurements (Popescu, 2007). Since the remotely sensed observations do not directly measure biomass, they use radiometry, which is sensitive to vegetation structure (crown size and tree density), texture and shadow and therefore can be correlated with AGB (Baccini et al., 2008). Optical and radar sensors have been used successfully in various studies (Saatchi and Moghaddam, 1995; Steininger, 2000; Baccini et al., 2004). Besides, lidar technology that emits laser pulses from the instrument towards a target and measures the reflected energy and/or time difference between the pulse emission and reception is used to relate the vertical distribution of canopy structure and consequently for estimation of AGB. It has been known that AGB models using airborne lidar metrics are significantly more accurate than those based on the satellite-bornes' while the spatial extent of airborne lidar is typically restricted to relatively smaller areas and data acquisition is rather expensive (Zolkos et al., 2013).

On the other hand, the satellite-based lidar, Geoscience Laser Altimeter System (GLAS) on Ice, Cloud, and Land Elevation Satellite (ICESat) provides information about the vertical structure of its "footprint" area of ~70 m diameter depending on intercepted surface area, orientation, surface reflectivity and the returned energy level changes in given height (Yavaşlı, 2016). The returned waveforms from the footprints of GLAS are used to estimate tree height, AGB, and basal area (Lefsky et al., 2005; Rosette et al., 2008), however accuracies depend on canopy density and terrain topography. AGB estimation models that uses GLAS data achieve promising results and can explain 55% to 74% of the field estimates (Zolkos

et al., 2013). However, the GLAS data usually requires data fusion with other imagery to extend geographic coverage.

This study demonstrates the use of GLAS and Landsat data to model AGB estimation at Calabrian pine forests of Düzleçamı, Antalya province of Turkey where no airborne lidar data is available. The innovation of the study is the use of satellite-based lidar, GLAS with the combination of optical sensor, Landsat. The goals of this study are (1) to create the biomass distribution map of the study area, (2) develop a method to model AGB from GLAS and Landsat integration and (3) to assess the relationship of GLAS parameters and Landsat data with biomass.

2. Study Area

The study area is the forest area at the south of Düzlerçamı sub-district directorate at Antalya province of Turkey (fig. 1). The forest area of 10500 ha is dominated with Calabrian pine (Pinus brutia). Topographical simplicity was the main criteria for the study area selection considering the bias of the GLAS data in complex topographies. Mediterranean climate is observed at the study area with hot, dry summers and warm, wet winters. The seasonal rainfall pattern is particularly distinctive, with virtually all of it falling during the winter months.

3. Data

We used GLAS data products GLA01, GLA06 and GLA14 of release 33 obtained from National Snow and Ice Data Center (NSIDC). IDL has been used to extract information contained in GLA01, GLA06 and GLA14. GLA01 and GLA06 waveforms are linked to GLA14 with the record and shot numbers. The quality flags such as "i_FRir_qaFlag" utilized to select cloud free shots.

Cloud and snow free Landsat image is needed to assess the pixel values of the study area. Landsat 8 Operational Land Imager (OLI) image of 12 August 2017 used to calculate various indices and correlate with the AGB. The acquisition date of the image also corresponds with the field data collection dates. The Landsat OLI image is calibrated and atmospherically corrected to surface reflectance by Earth Resources Observation and Science (EROS) data center using the MODIS 6S radiative transfer approach.

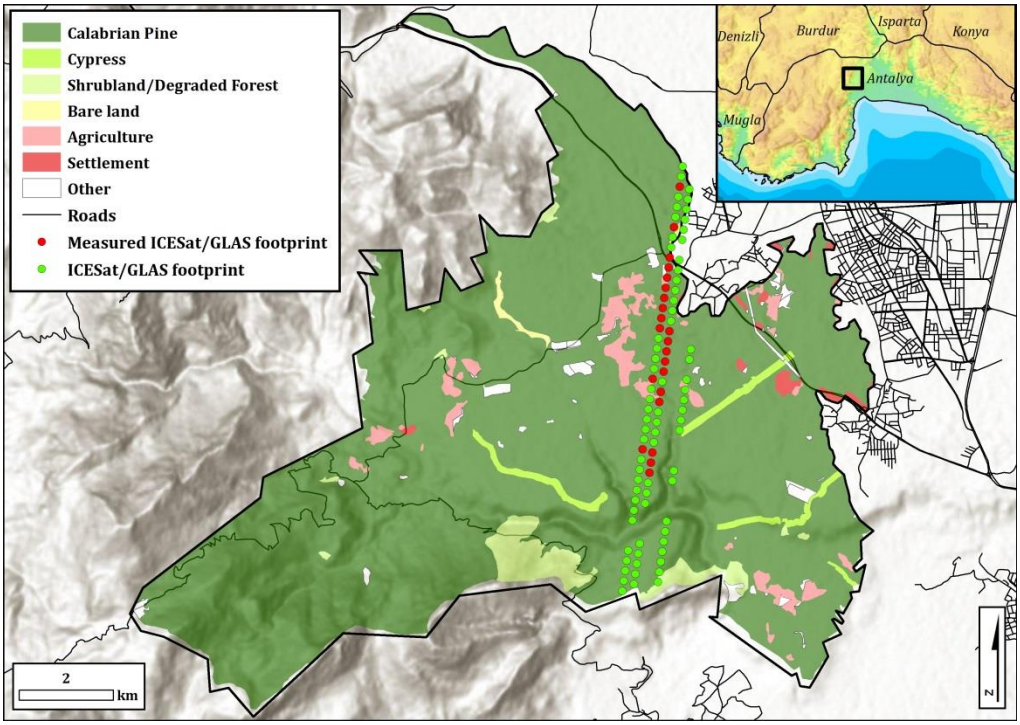

Figure 1- The location and simplified stand map of the study area with ICESat/GLAS footprints.

The field data was collected in August 2017. Diameter at breast height was measured for every tree within a 10 m diameter for 22 plots within the study area. The plots were positioned using a Magellan eXplorist Pro 10 handheld GPS with a horizontal accuracy about 2-5 m.

4. Methodology

Various parameters including signal begin range offset (SigBegOff), signal end range offset (SigEndOff), centroid range increment for gaussian fits (gpCntRngOff), the peaks of first two gaussian amplitudes (gamp), centroid range offset (cntRngOff), cloud flag (FRir_qaFlag), saturation index (satNdx) has been extracted from the GLAS data using GLAS Visualizer for IDL. One of the most important parameter needed to calculate is the height of the Gauss peak that represents the return signal from ground. Even though the peak of the first Gaussian "usually" represents the ground return for flat surfaces it has been found that in some cases where the terrain is complex, the second Gaussian peak might represent ground return (Rosette et al., 2008). We preferred to use the waveform of either Gaussian peak # 1 or 2 whichever demonstrated the greater amplitude to determine the ground return.

Wide range of studies have shown that the height of median energy (HOME) metric is sensitive to both the vertical arrangement and density of forest canopy making it to be useful predictor of biomass. In areas with dense forest less GLAS energy is likely to reach the ground causing HOME metric to increase; conversely in open areas more energy reaches the ground and reduces HOME (Drake et al. 2002). The HOME metric we used in this study is calculated using the difference of centroid range offset and ground return. We also calculated the ratio of HOME to maximum vegetation height (%HOME).

Using the geolocation data of GLA14 data product the calculated parameters were exported to ArcGIS 10.4 software. We removed the footprints that fall on the areas having more than 15° of slope, the ones at the non-forest areas and the ones with extreme values due to cloud and other conditions. Ninety-four available GLAS footprints have been determined at the study area (fig. 1).

Optical data and various vegetation indices derived from it has been widely used for AGB estimation (Saatchi et al., 2007; Lu et al., 2004; Dong et al., 2003). The correlations of these indices with AGB vary depending on many issues such as seasonality, background effects and species (Yavaşlı, 2016). In this study, we used 26 vegetation indices that are widely mentioned to be interrelated with AGB to create biomass distribution map of the study area (see Appendix). ENVI 5.0 software is used to create the indices.

The Landsat indices pixel values were combined with the GLAS footprint data using ArcGIS 10.4. The GLAS shots coincide with a single Landsat pixel. However, the shots are usually affected from the neighbor pixels. To overcome this issue, bilinear interpolation have been used in calculation of Landsat OLI pixel values on GLAS footprints.

Because of the fact that the forests of the study area is comprised of Calabrian pine, the equation of Sun et al. (1980) has been used to calculate the AGB of each individual tree (eq. 1).

$$AGB\ (kg/tree) = 0.128 \times d^{2.267} \quad (1)$$

Where d is the diameter at breast height. All the individual tree biomass values at the field plots were then converted to AGB per hectare.

Multiple linear regression analysis was used to model the relationship between AGB values collected from field, GLAS and Landsat OLI data. Multiple linear regression is a technique that estimates a single regression model with more than one outcome variable (Yavaşlı, 2016).

In the first model ($Model_A$) HOME and %HOME parameters of 22 GLAS plots were used as independent variables while AGB estimates from the field data is used as dependent variable. AGB estimates of GLAS data that has been obtained from $Model_A$ is used as dependent variable; Landsat OLI pixel values of each bands and pixel values of the indices are used as independent variable in the second model ($Model_B$). In the third model ($Model_C$) Landsat OLI pixel values of each bands and pixel values of the indices are used as independent variable where dependent variables are AGB estimates from the field data.

The dependent variable can be explained using either all of the independent variables or only the more related ones in multiple linear regression. The adjusted R^2, which is a modified version of R^2 and gives the percentage of variation explained by only those independent variables that in reality affect the dependent variable, is used for the selection of the model.

5. Results and Discussion

5.1 Model$_A$ – Biomass and ICESat

Variance analysis results (table 1) show that HOME and %HOME parameters are related with AGB having a R^2 of 0.87 (fig. 2) and this relationship is statistically significant given the fact that the probability corresponding to the F value is lower than 0.01 (table 2). Model$_A$ explaining the AGB estimation using GLAS data is as follows:

$$\text{AGB ModelA} = 21.18 + 44.92 * \text{HOME} - 6.27 * \%\text{HOME} \quad (2)$$

5.2 Model$_B$ – ICESat and Landsat

Model$_B$ uses the AGB estimations using Model$_A$ for 94 GLAS shots and 26 variables obtained from Landsat OLI indices and pixel values of each bands. The selected model that has the highest adjusted R^2 uses 13 variables (table 3) and is as follows:

$$\text{AGB – ModelB} = -24115 - 8631 * \text{ARVI} - 3.54 * \text{EVI} - 48.76 * \text{L5} - 9212 * \text{ND53} + 2041 * \text{RSR} - 42394 * \text{SAVI} + 2.08 * \text{TC2} - 0.53 * \text{TC3} + 12067 * \text{TM43} + 13270 * \text{TM53} - 20514 * \text{TM54} - 1304 * \text{TM57} + 0.92 * \text{VIS123} \quad (3)$$

Variance analysis results (table 3) and variables selection table (table 4) show that the selected parameters of Landsat are related with AGB having a R^2 of 0.52 (Fig. 7) and this relationship is statistically significant given the fact that the probability corresponding to the F value is lower than 0.01. However, it is considered that the R^2 is insufficient to explain the AGB.

5.3 Model$_C$ – Biomass and Landsat

Model$_C$ uses the AGB estimates from the field data and 26 variables obtained from Landsat OLI indices and pixel values of each bands. Variance analysis results (table 5) show that 11 parameters of Landsat OLI (table 6) are related with AGB having a R^2 of 0.91. This relationship is statistically significant given the fact that the probability corresponding to the F value is lower than 0.01 (table 7). The equation is as follows:

$$\text{AGB - Model}_C = -736767 - 97{,}59 * \text{L2} - 98{,}50 * \text{L3} - 45221 * \text{ND53} - 81734 * \text{ND54} - 1409539 * \text{ND57} - 10{,}62 * \text{TC2} + 2{,}35 * \text{TC3} + 101078 * \text{TM53} - 56462 * \text{TM54} + 526452 * \text{TM57} + 5{,}71 * \text{VIS123} \quad (4)$$

Using the equation 4 and "band math" in ENVI, we have created the AGB distribution map of study area (fig. 5). The non-forest areas are masked using NDVI threshold of 0.2. It may be observed that the higher biomass values generally take part on the northern of the study area. Most of the biomass values range between 50-200 t/ha.

Table 1- Summary of the variables selection for Model$_A$. Selected model variables are shown bold.

# of variables	Variables	MSE	R^2	Adjusted R^2
1	HOME	2917,53	0.78	0.77
2	**HOME / RH50**	1857,23	0.87	**0.85**

Table 2- Analysis of variance for Model$_A$.

	Degree of freedom	Sum of squares	Mean squares	F	Pr > F (Sig.)
Model	2	236485.02	118242.51	63.66	< 0.0001
Error	19	35287.46	1857.23		
Corrected Total	21	271772.49			

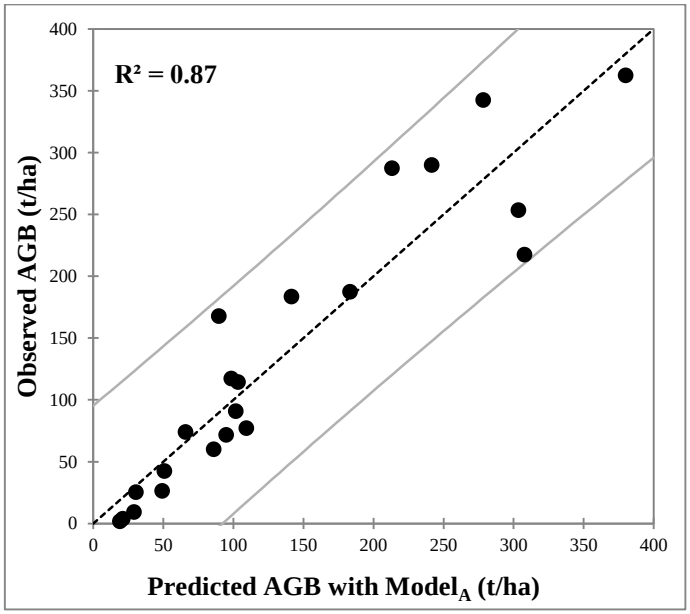

Figure 2- Observed vs predicted AGB using Model$_A$.

Table 3: Summary of the variables selection for Model$_B$. Selected model variables are shown bold.

# of variables	Variables	MSE	R^2	Adjusted R^2
10	ARVI / EVI / GEMI / L5 / RSR / TC1 / TM53 / TM54 / TM57 / VIS123	3884.21	0.50	0.44
11	ARVI / EVI / GEMI / L5 / ND32 / RSR / TC3 / TM53 / TM54 / TM57 / VIS123	3861.64	0.51	0.44
12	EVI / L5 / L7 / ND57 / RSR / SAVI / TC2 / TM43 / TM53 / TM54 / TM57 / VIS123	3811.41	0.52	0.45
13	**ARVI / EVI / L5 / ND53 / RSR / SAVI / TC2 / TC3 / TM43 / TM53 / TM54 / TM57 / VIS123**	**3810.85**	**0.52**	**0.45**

Table 4: Analysis of variance for Model$_B$.

	Degree of freedom	Sum of squares	Mean squares	F	Pr > F (Sig.)
Model	13	341739.21	26287.63	6.89	< 0.0001
Error	80	304868.44	3810.85		
Corrected Total	93	646607.65			

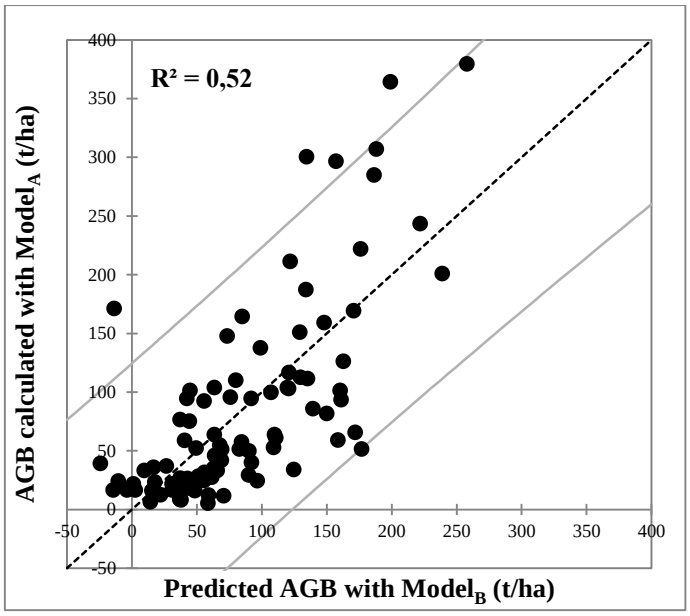

Figure 3: AGB calculated with Model$_A$ vs predicted AGB using Model$_B$

Table 5: Table 4: Analysis of variance for Model$_C$.

	Degree of freedom	Sum of squares	Mean squares	F	Pr > F (Sig.)
Model	11	247979.78	22543.61	9.47	0.0007
Error	10	23792.70	2379.27		
Corrected Total	21	271772.49			

Table 6: Summary of the variables selection for Model$_C$. Selected model variables are shown bold.

# of variables	Variables	MSE	R²	Adjusted R²
9	L2 / L3 / ND54 / ND57 / TC2 / TM53 / TM54 / TM57 / VIS123	3300.60	0.85	0.74
10	L2 / L3 / ND54 / ND57 / TC2 / TC3 / TM53 / TM54 / TM57 / VIS123	2381.75	0.90	0.81
11	**L2 / L3 / ND53 / ND54 / ND57 / TC2 / TC3 / TM53 / TM54 / TM57 / VIS123**	**2379.27**	**0.91**	**0.81**

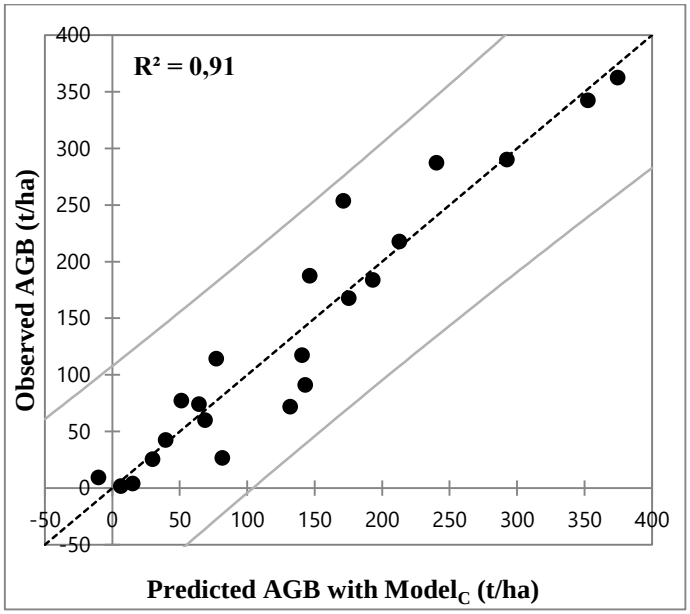

Figure 4: Observed vs predicted AGB using Model$_C$.

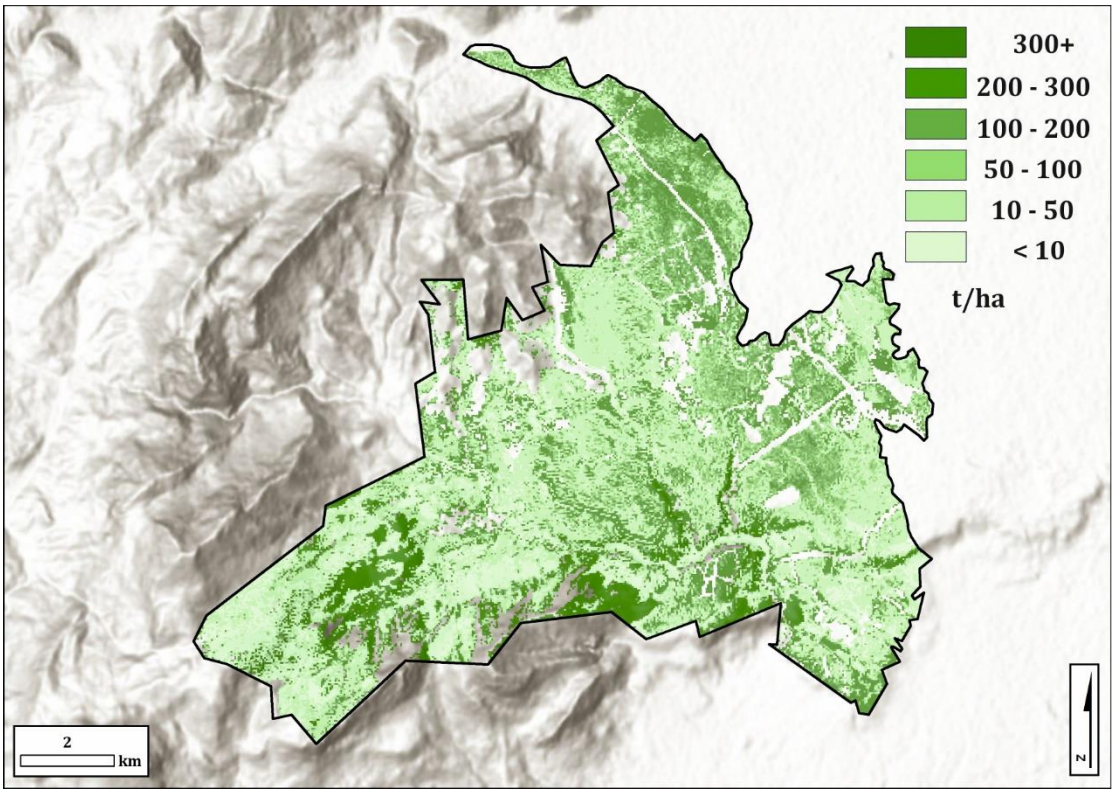

Figure 5: AGB distribution of the study area.

6. Conclusion

This study depictures the use of remotely sensed data of Landsat and GLAS for AGB estimation. $Model_A$ shows that there is a statistical relationship between AGB and HOME and %HOME metrics derived from GLAS data with a R^2 of 0.87 however $Model_B$ indicated that the these metrics cannot be statistically related to Landsat data and various vegetation indices since the R^2 value is 0.52. The most of the AGB models based on GLAS data in literature explained the variability between 0.55–0.74 (Zolkos et al., 2013). The same method has been implemented in a different part of Turkey and had better results with a R^2 of 0.73 (Yavaşlı, 2016). On the other hand, a better statistical relationship has been found with Landsat data and AGB with a R^2 of 0.91 in $Model_C$. Using this model the AGB distribution map of study area, the Calabrian pine forests of Düzlerçamı, is created.

The study succeeded to achieve encouraging results in estimation of AGB however, we acknowledge that there are some issues that needs to be improved. It is very clear that there is a considerable change in forest condition between the acquisition of GLAS data and fieldwork and Landsat data acquisition dates. This might be the major reason for ineffectualness of $Model_B$. Another issue is the effect of topography at the southeastern part of the study area. It may be noticed that there is a distinct AGB highness at the sides of the valley. This is somehow unexpected since the Landsat data is terrain corrected. The aspect effect might be the reason for higher biomass values and it needs to be verified with additional fieldwork.

7. Acknowledgements

This work was supported by Ege University Scientific Research Projects Coordination Unit (grant number 16-EDB-012). We would like to thank to the staff of general directorate of forestry at Düzlerçamı for their cooperation at the field work.

REFERENCES

Baccini A., Friedl M.A., Woodcock C.E., Warbington R., 2004. Forest biomass estimation over regional scales using multisource data. *Geophysical Research Letters*, 31, L10501, doi: 10.1029.

Baccini A., Laporte N., Goetz S. J., Sun M., Dong H., 2008. A First Map of Tropical Africa's Above-ground Biomass Derived from Satellite Imagery, *Environmental Research Letters*, 3(4).

Birth, G. S., & McVey, G. R., 1968. Measuring the color of growing turf with a reflectance spectrophotometer. *Agronomy Journal*, *60*(6), 640-643.

Brown L., Chen J. M., Leblanc S. G., Cihlar J., 2000. A shortwave infrared modification to the simple ratio for LAI retrieval in boreal forests: An image and model analysis. *Remote sensing of environment*, *71*(1), 16-25.

Brown, S., 1997. Estimating biomass and biomass change of tropical forests: a primer (Vol. 134). Food & Agriculture Org..

Chambers, J. Q., Higuchi N., Teixeira L. M., Santos J. D., Laurance S. G., Trumbore S. E., 2004. Response of tree biomass and wood litter to disturbance in a Central Amazon forest, *Oecologia*, 141, 596 – 614.

Chave, J., Réjou-Méchain, M., Búrquez, A., Chidumayo, E., Colgan, M. S., Delitti, W. B., ... & Henry, M. (2014). Improved allometric models to estimate the aboveground biomass of tropical trees. *Global change biology*, 20(10), 3177-3190.

Crist E. P., Cicone R,. 1984. Application of the Tasseled Cap Concept to Simulated Thematic Mapper Data, *Photogrammetric Engineering and Remote Sensing*, 50, 343-352.

Dong J., Kaufmann R.K., Myneni R.B., Tucker C.J., Kauppi P.E., Liski J., Buermann W., Alexeyev V., Hughes M.K., 2003. Remote sensing estimates of boreal and temperate forest woody biomass: carbon pools, sources, and sinks. *Remote Sensing of Environment*, 84, 393–410.

Drake, J.B., Dubayah, R.O., Clark, D.B., Knox, R.G., Blair, J.B., Hofton, M.A., Prince, S., 2002. Estimation of tropical forest structural characteristics using large-footprint lidar. *Remote Sensing of Environment*. 79 (2), 305–319.

Foody G. M., Boyd D. S. Cutler M. E. J., 2003. Predictive relations of tropical forest biomass from Landsat TM data and their transferability between regions. *Remote Sensing of Environment*, 85(4), 463-474.

Huete A. R., Liu H., Batchily K., van Leeuwen W., 1997. A Comparison of Vegetation Indices Over a Global Set of TM Images for EOS-MODIS. *Remote Sensing of Environment*, 59 (3), 440-451.

Huete A.R, 1998., A soil-adjusted vegetation index (SAVI), *Remote Sensing of Environment*, 25 (3), 295-309.

Kaufman Y. J., Tanre D., 1996. Strategy for Direct and Indirect Methods for Correcting the Aerosol Effect on Remote Sensing: from AVHRR to EOSMODIS. *Remote Sensing of Environment*. 55, 65-79.

Lefsky, M.A., Harding, D.J., Keller, M., Cohen, W.B., Carabajal, C.C., Espirito-Santo, D.B., F, Hunter, M.O., de Oliveira, R., Jr., 2005. Estimates of forest canopy height and aboveground biomass using ICESat. *Geophysical Research Letters*, 32.

Lu D., Mausel P., Brondizio E., Moran E., 2002. Above-Ground Biomass Estimation of Successional and Mature Forests Using TM Images in the Amazon Basin. *Symposium on Geospatial Theory, Processing and Applications*.

Lu D., Mausel P., Brondizio E., Moran E., 2004. Relationships Between Forest Stand Parameters and Landsat TM Spectral Responses in the Brazilian Amazon Basin. *Forest Ecology and Management*, 198 (1-3), 149–167.

Pinty B., Verstraete M. M., 1992. GEMI: a Non-linear Index to Monitor Global Vegetation from Satellites, *Plant Ecology*, 101 (1), 15-20.

Popescu, S. C., 2007. Estimating biomass of individual pine trees using airborne lidar. *Biomass and Bioenergy*, 31(9), 646-655.

Qi J., Chehbouni A., Huete A. R., Kerr Y. H., Sorooshian S., 1994a. A Modified Soil Adjusted Vegetation Index, *Remote Sensing of Environment*, 48 (2), 119-126.

Qi J., Kerr Y., Chehbouni A., 1994b. External factor consideration in vegetation index development. *Proc. of Physical Measurements and Signatures in Remote Sensing, ISPRS*, 723-730.

Rosette, J.A.B., North, P.R.J., Suarez, J.C., 2008. Vegetation height estimates for a mixed temperate forest using satellite laser altimetry. *International Journal of Remote Sensing*. 29 (5), 1475–1493.

Saatchi S. S., Houghton R. A., Dos Santos Alvalá R. C., Soares J. V., Yu Y., 2007. Distribution of Aboveground Live Biomass in the Amazon Basin, *Global Change Biology*, 13 (4), 816–37.

Saatchi S. S., Moghaddam M., 1995. Biomass of Boreal Forest Using Polarimetric SAR Imagery. *Geoscience and Remote Sensing, IEEE Transactions*, 38(2), 697-709.

Steininger M. K., 2000. Satellite estimation of tropical secondary forest aboveground biomass: data from Brazil and Bolivia. *International Journal of Remote Sensing*, 21, 1139–1157.

Sun O., Uğurlu S., Özer E., 1980. Kızılçam (Pinus brutia Ten.) türüne ait biyolojik kütlenin saptanması. *Ormancılık Araştırma Enstitüsü Teknik Bülteni*, Teknik Bülten Serisi No: 104.

Tucker C. J., 1979. Red and Photographic Infrared Linear Combinations for Monitoring Vegetation. *Remote Sensing of Environment*, 8, 127-150.

Yavaşlı, D. D., 2016. Estimation of above ground forest biomass at Muğla using ICESat/GLAS and Landsat data. *Remote Sensing Applications: Society and Environment*, *4*, 211-218.

Zolkos, S.G., Goetz, S.J., Dubayah, R., 2013. A meta-analysis of terrestrial aboveground biomass estimation using lidar remote sensing. *Remote Sensing of Environment*. 128, 289–298.

Appendix A: The list of the vegetation indices used

ABBREVIATION	DEFINITION	REFERENCE
ALB	Albedo	Lu et al. 2002
ARVI	Atmospherically Resistant Vegetation Index	Kaufman and Tanre 1996
ASVI	Atmosphere Soil Vegetation Index	Qi et al., 1994a
EVI	Enhanced Vegetation Index	Huete et al., 1997
GEMI	Global Environmental Monitoring Index	Pinty and Verstraete 1992
MSAVI	Modified Soil Adjusted Vegetation Index	Qi et al., 1994b
ND32	Normalized Difference Index	Foody et al. 2003; Lu et al. 2004
ND53	Normalized Difference Index	Foody et al. 2003; Lu et al. 2004
ND54	Normalized Difference Index	Foody et al. 2003; Lu et al. 2004
ND57	Normalized Difference Index	Foody et al. 2003; Lu et al. 2004
NDVI	Normalized Difference Vegetation Index	Tucker 1979;
R271	Complex Ratio	Foody et al. 2003;
R327	Complex Ratio	Foody et al. 2003;
RSR	Reduced Simple Ratio	Brown et al. 2000
SAVI	Soil Adjusted Vegetation Index	Huete 1988
TM57	Simple Ratio	Lu et al. 2004
TM54	Simple Ratio	Lu et al. 2004
TM53	Simple Ratio	Lu et al. 2004
TM43	Simple Ratio	Birth and McVey 1968
VIS123	Visible Bands	
TC1	Tasseled Cap Brightness	Crist and Cicone 1984
TC2	Tasseled Cap Greenness	Crist and Cicone 1984
TC3	Tasseled Cap Wetness	Crist and Cicone 1984
TC4	Tasseled Cap Forth	Crist and Cicone 1984
TC5	Tasseled Cap Fifth	Crist and Cicone 1984
TC6	Tasseled Cap Sixth	Crist and Cicone 1984